Recent development in aluminum alloys

PURE ALUMINIUM

Annealed pure aluminium is:

- not very strong
- soft and ductile
- light in weight
- corrosion resistant
- of high thermal and electrical conductivities

Typical mechanical properties are:

	Annealed	Moderate cold work
0.2% Yield Strength	15 MPa	50 MPa
UTS	50 MPa	100 MPa
Elongation †	50%	50%
Hardness	130 Hv	230 Hv

† maximum elongation before breaking

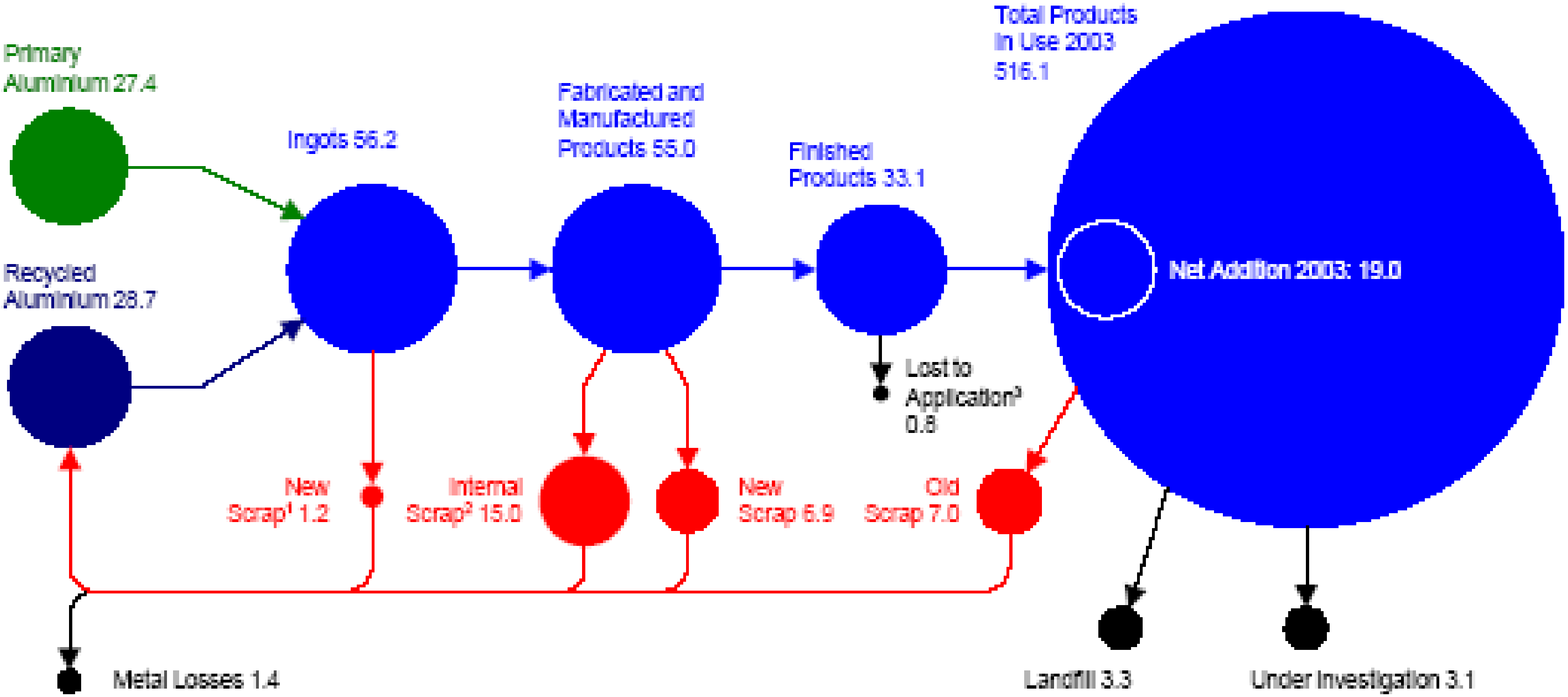

Values in millions of metric tonnes.
Values might not add up due to rounding.
1 Skimmings, scalpings, sawings
2 Not taken into account in statistics
3 Such as powder, paste and deoxidation aluminium
4 Area of current research to identify final aluminium destination (reuse, recycling or landfilling)

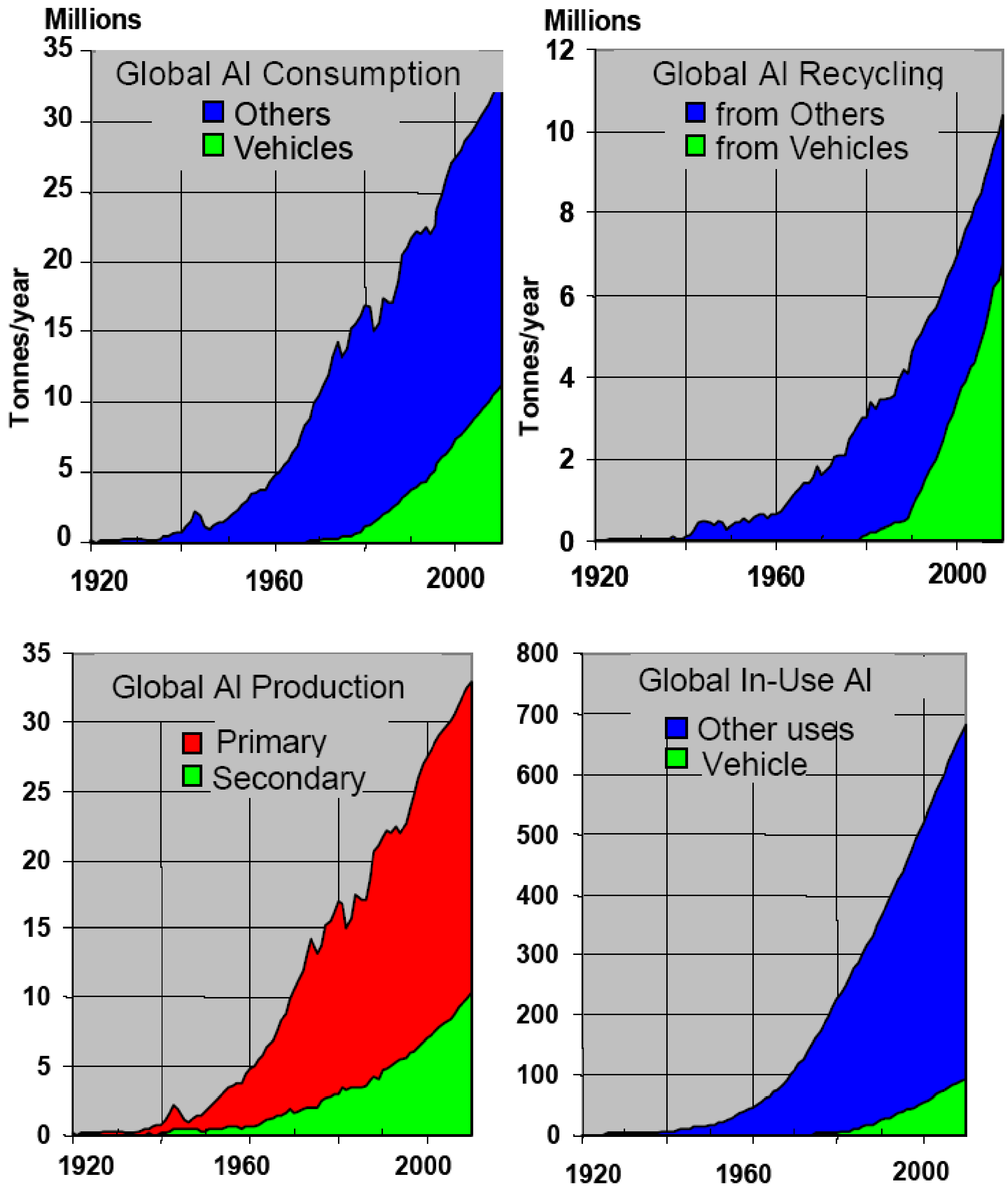

Figure 1: Global Al consumption, production, recycling and the vehicle share of the Al market

Sheet Al cars

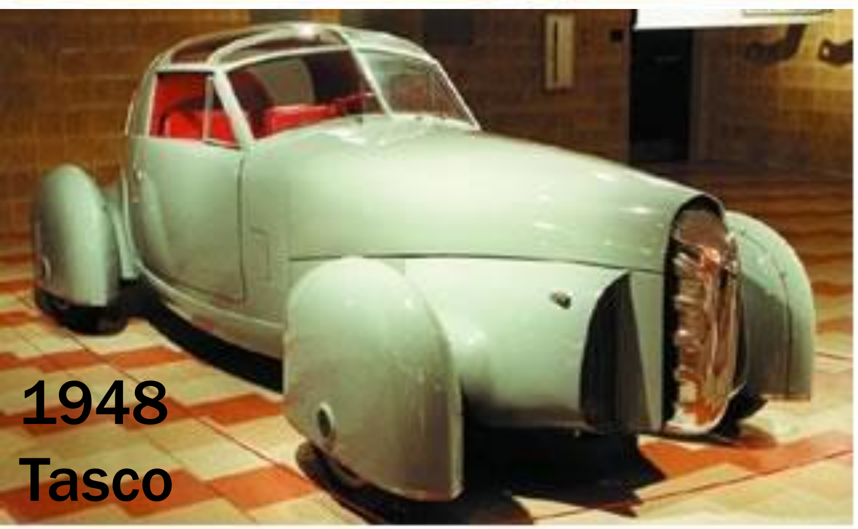

Wrought, heat-treatable aluminium alloys

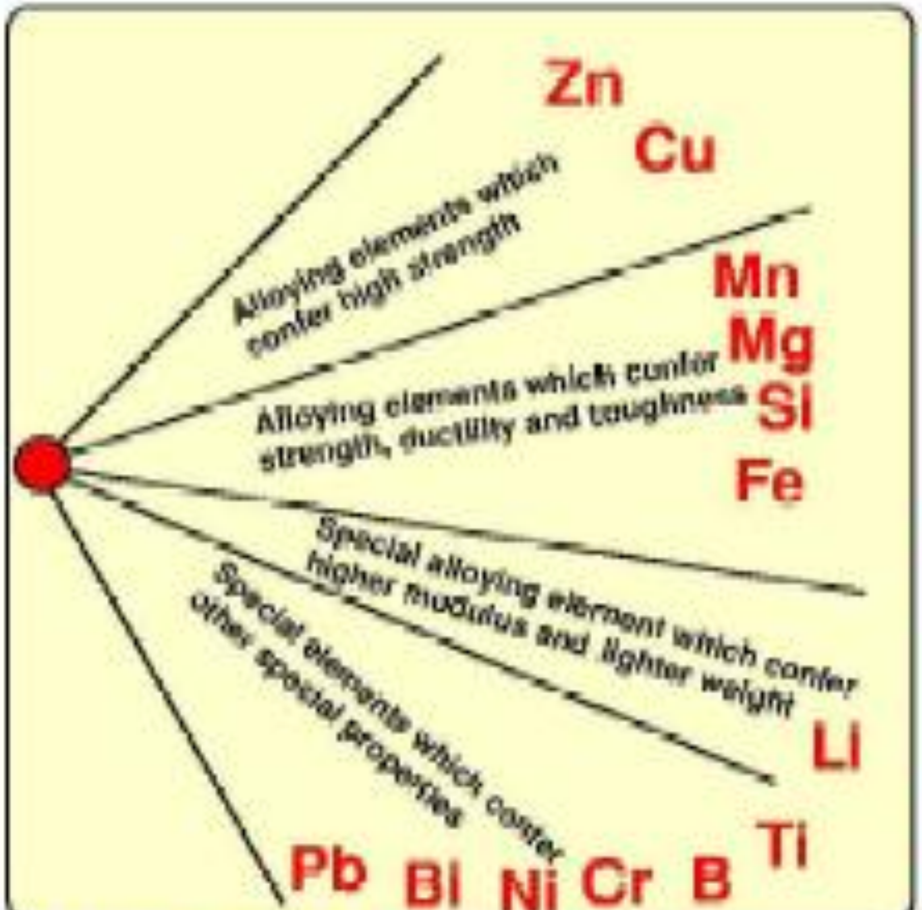

Al - Cu

- Pb and Bi (both insoluble in al) added to improve machinability
- Mg and Zn added to improve strength
- Ni and Fe added to form intermetallic which inhibits recrysatilisation and grain growth
- Zr added to pin grain boundaries and retain very small grain size essential for superplastic deformation
- Li added for increased modulus and lighter weight for aerospace applications

Al - Mg - Si

- Cu added to offset delayed ageing effect
- Cr added to enhance corrosion properties
- excess Si added to enhance tensile properties

Al - Zn - Mg

- Cu added to obtain very high strength

Wrought aluminium alloy compositions

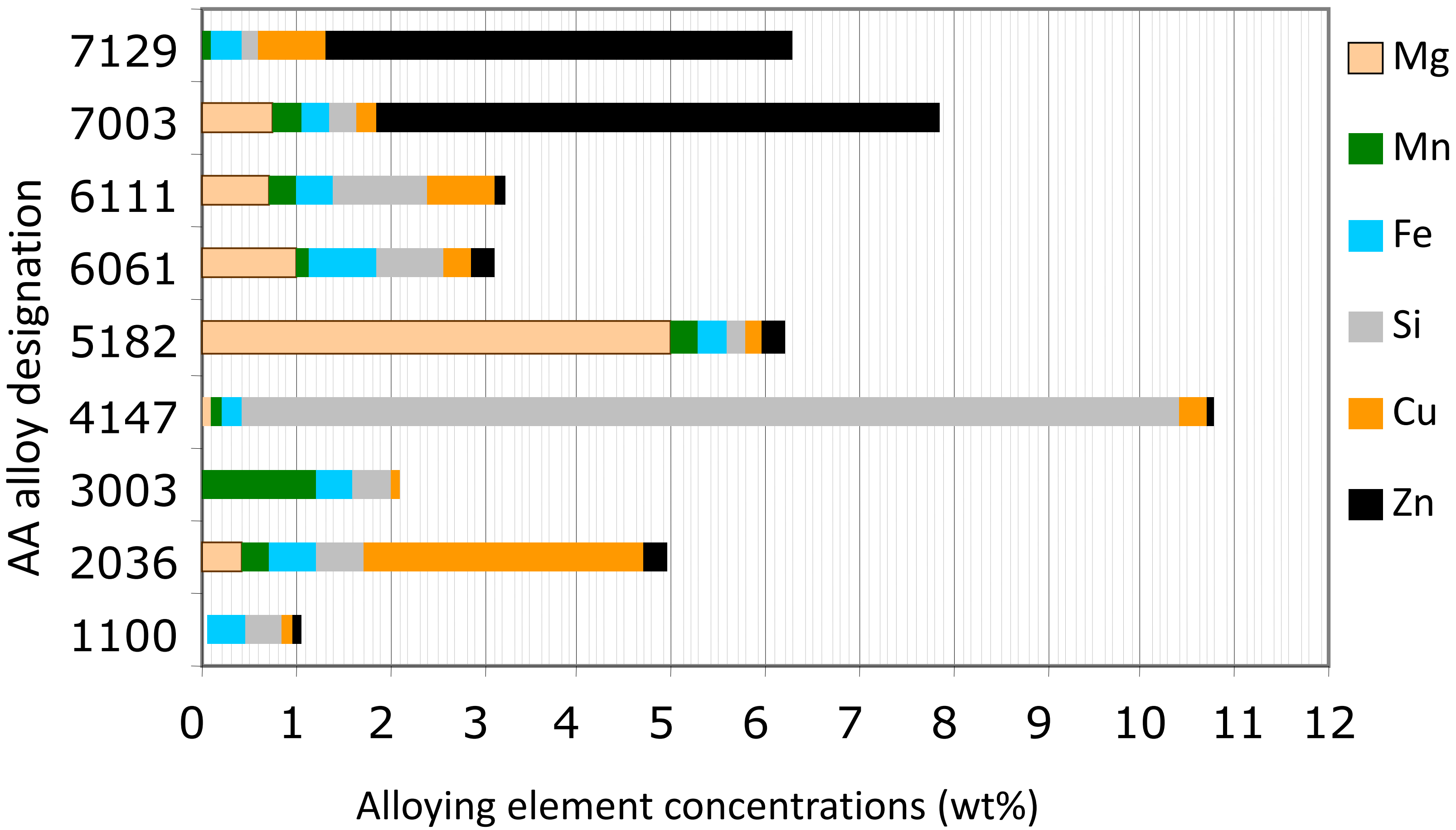

Cast aluminium alloy compositions

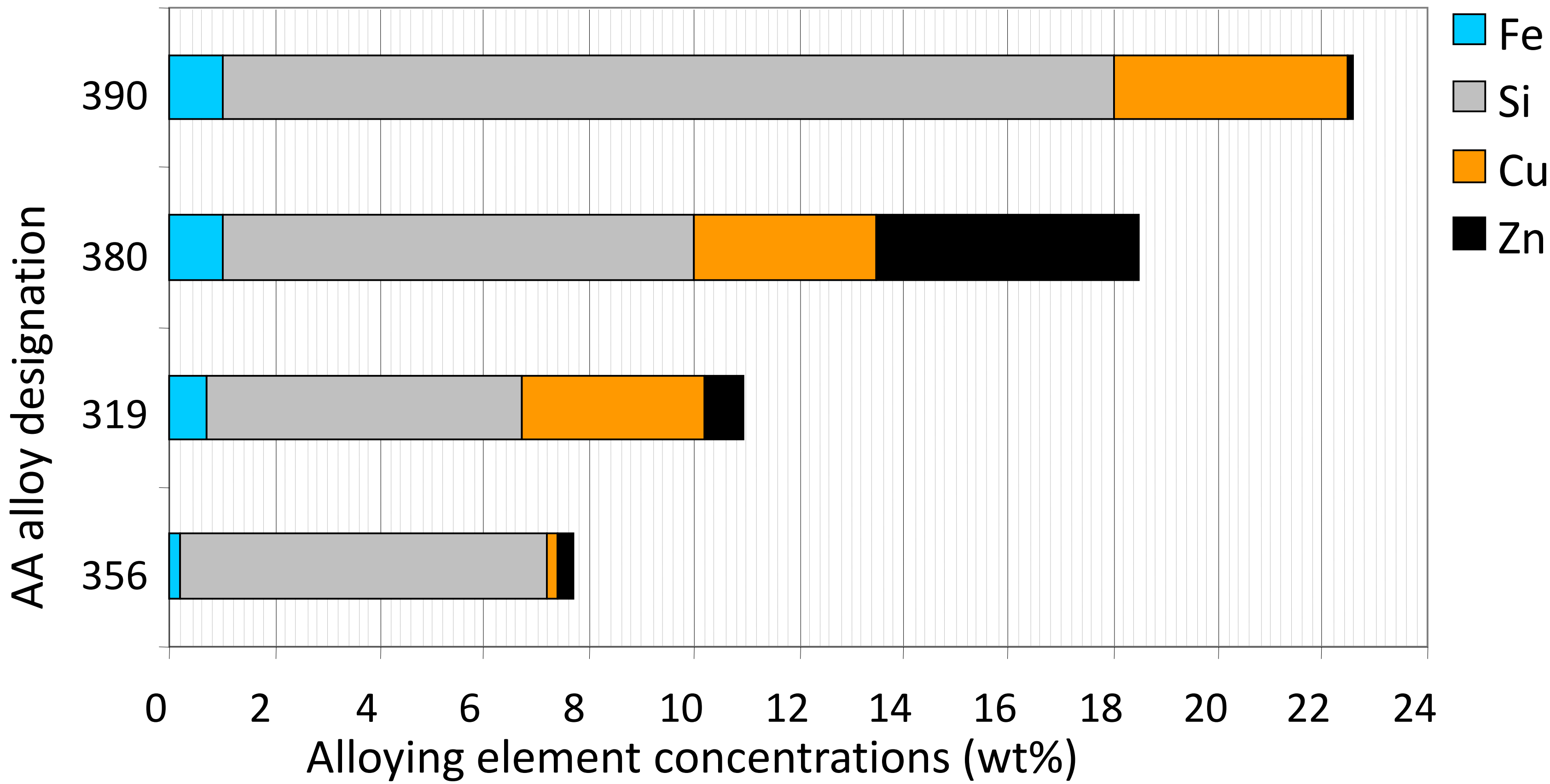

Table 3: American Aluminum Association maximum concentration limits of common automotive alloys and key secondary alloys in other major Al markets*

AA Alloy	Si	Cu	Mg	Mn	Zn	Fe	Other
Transportation							
A319.0	6.5	4.0	0.1	0.5	3.0	1.0	
356.0	7.5	0.25	0.45	0.35	0.35	0.6	
A356.2	7.5	0.1	0.45	0.005	.005	0.12	
380.0**	**9.5**	**4.0**	**0.1**	**0.5**	**3.0**	**2.0**	
384.0**	**12.0**	**4.5**	**0.1**	**0.5**	**1.0**	**1.0**	**Ni 0.5**
390.0	18.0	5.0	0.65	0.1	0.1	0.5	
1100	0.5	0.2			0.1	0.5	
3003	0.6	0.2		1.5	0.1	0.7	
4032	13.5	1.3	1.3		0.25	1	Ni 1.3
5052	0.25	0.1	2.8	0.1	0.1	0.4	
5454	0.25	0.2	3.0	1.0	0.25	0.4	
5754	0.4	0.1	3.6	0.5	0.2	0.4	
5182	0.2	0.15	5.0	0.5	0.25	0.35	
6008	0.9	0.3	0.7	0.3	0.2	0.35	
6060	0.6	0.1	0.6	0.1	0.15	0.3	
6061	0.8	0.4	1.2	0.15	0.25	0.7	
6022	1.5	0.11	0.7	0.1	0.25	0.2	
6111	1.1	0.9	1.0	0.45	0.15	0.4	
6181A	1.1	0.25	1.0	0.4	0.3	0.5	
6016	1.5	0.2	0.6	0.2	0.2	0.5	
6082	1.3	0.1	1.2	1.0	0.2	0.5	
7003	0.3	0.2	1.0	0.3	6.5	0.35	
7108	0.1		1.4		5.5	0.1	
EN AC-51400DF	2		5	1			
Packaging							
3004/3104**	0.6	0.25	1.3	1.5	0.25	0.8	
Building products							
3105**	0.6	0.3	0.8	0.8	0.4	0.7	

*http://www.matweb.com, **secondary alloys

typical manufacturing scheme for AA6XXX body sheet

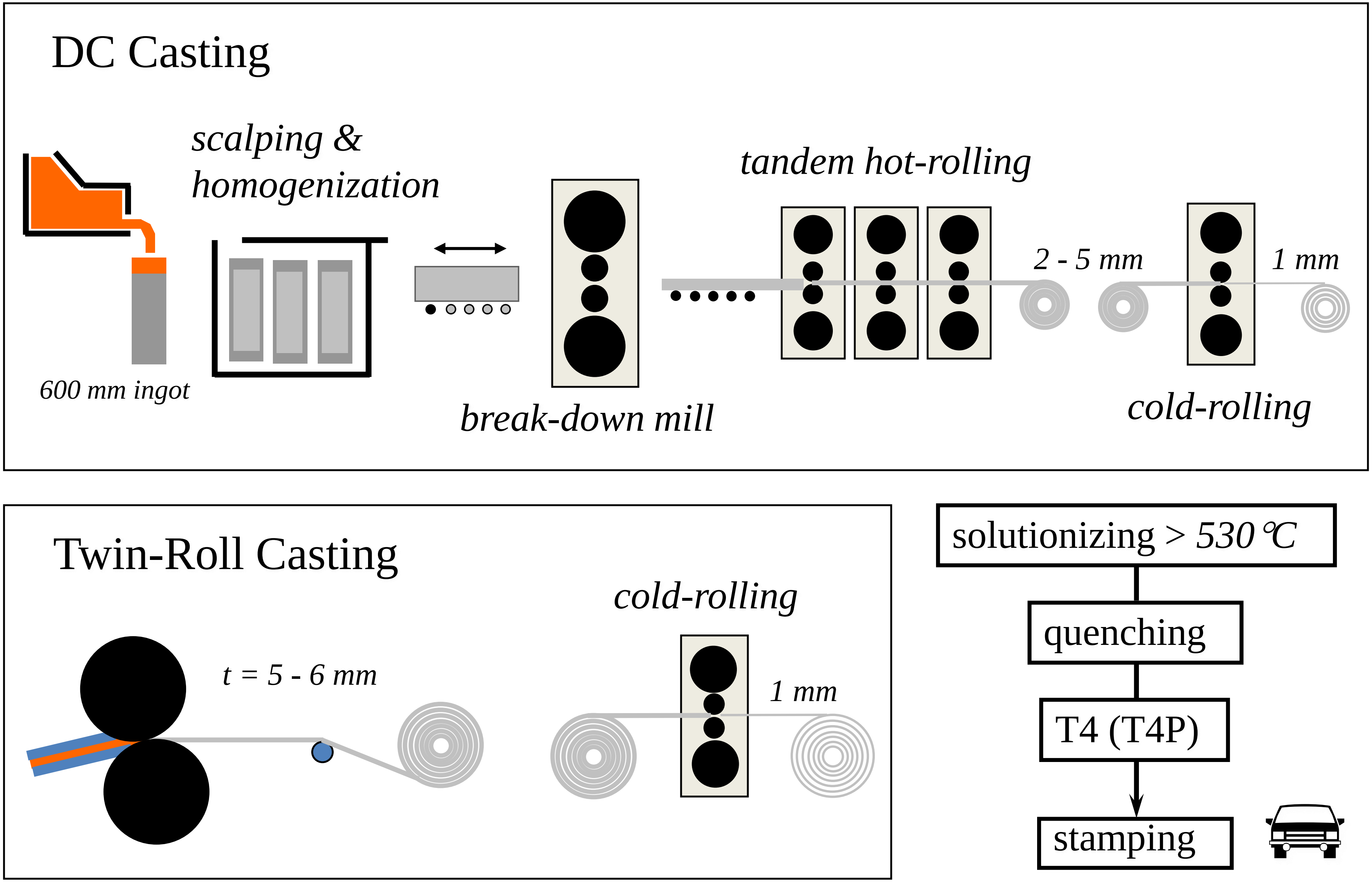

Thin-gauge wide strip casting

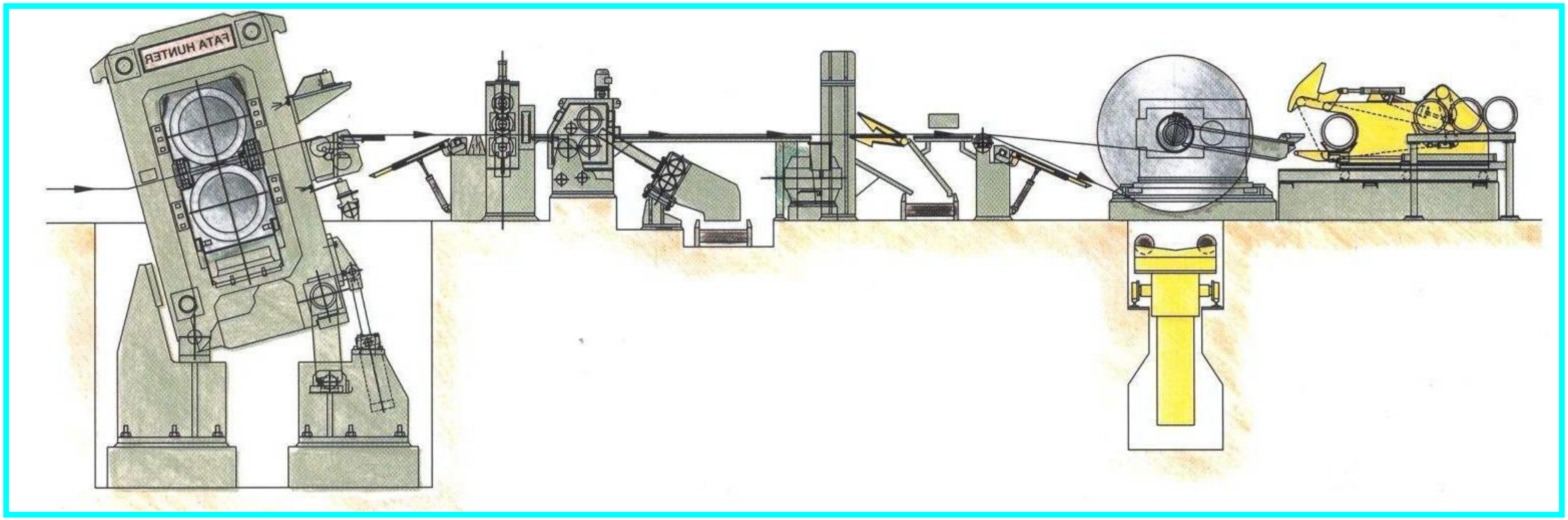

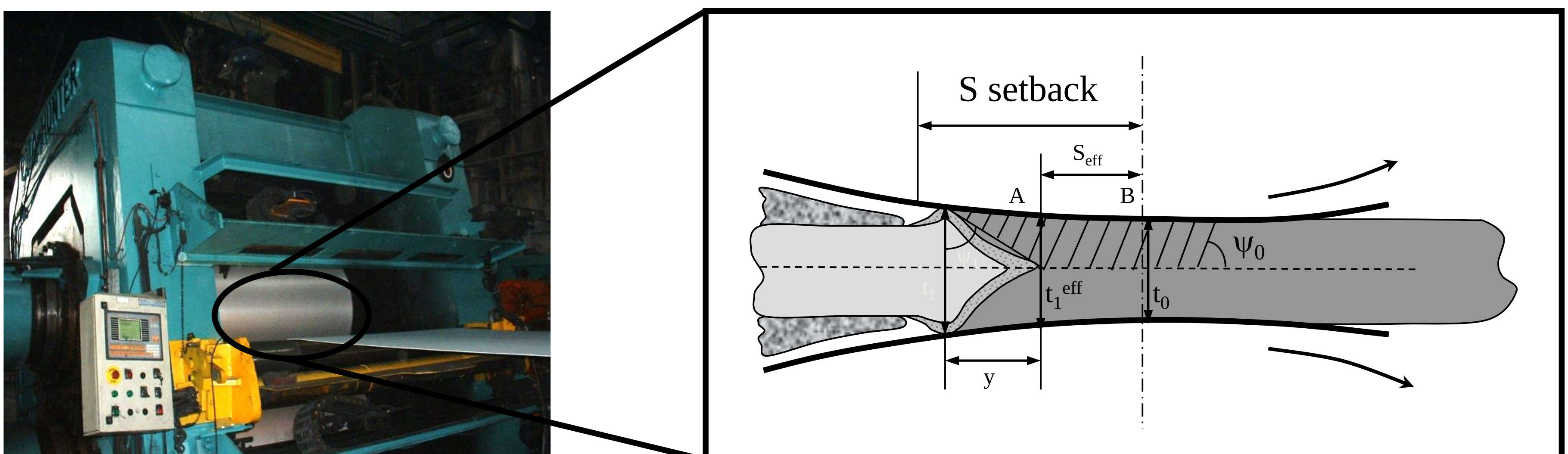

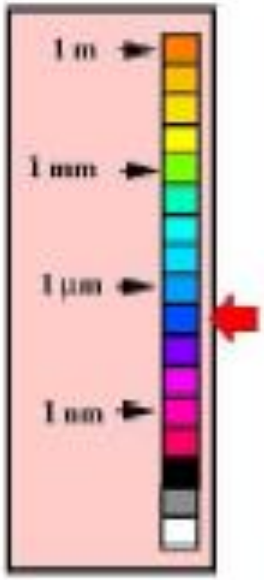

DIAGRAMS OF GP ZONES

Al - Cu   Al - Zn   Al - Mg_2Si

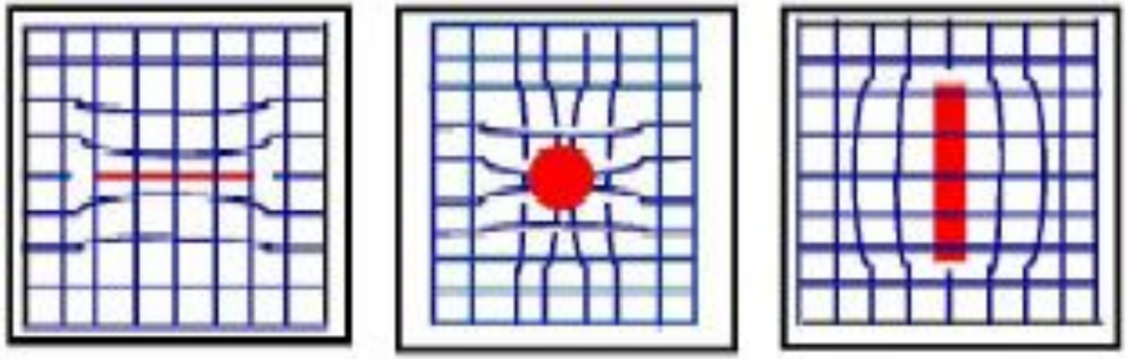

(a) Platelet on (100) cube plane

(b) Sphere

(c) Rod along [100] direction

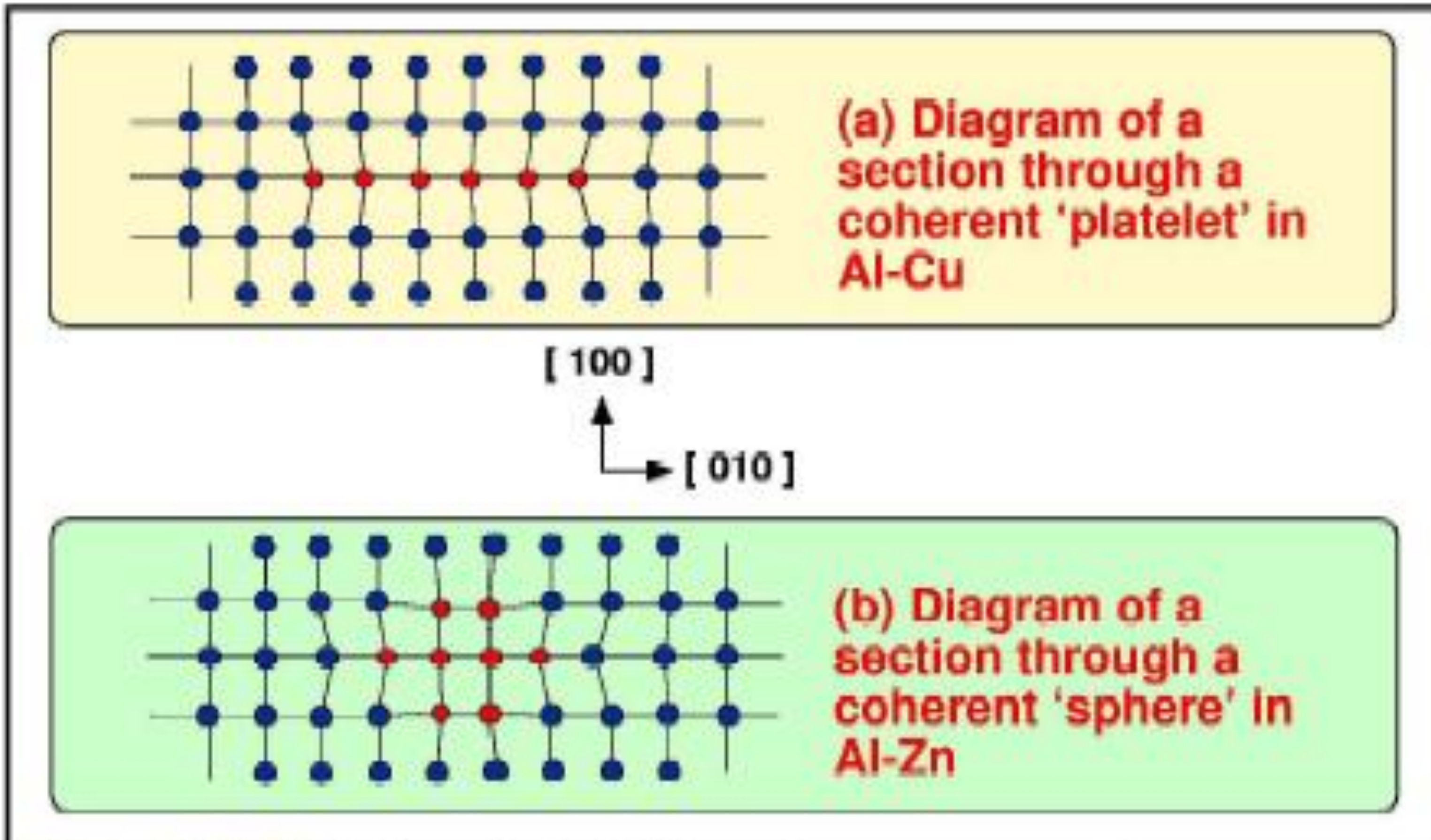

TALAT

Coherency in a cubic lattice;
[001] section of GP zone in Al-Cu and Al-Zn

1204.03.07

V	=	volume of solute cluster
A	=	surface area of solute cluster
r	=	radius of solute cluster
γ	=	interfacial surface energy of cluster per unit area
ΔG	=	total change in free energy per unit volume of cluster
ΔG_v	=	change in volume free energy per unit volume
ΔG_s	=	change in misfit strain energy per unit volume

$$\Delta G = -V\Delta G_v + V\Delta G_s + A\gamma$$

which becomes for a spherical cluster

$$\Delta G = -\frac{4}{3}\Pi r^3 (\Delta G_v - \Delta G_s) + 4\Pi r^2\gamma$$

and

$$\Delta G_{critical} = \frac{16\Pi\gamma^3}{3(\Delta G_v - \Delta G_s)^2} \qquad r_{critical} = \frac{2\gamma}{(\Delta G_v - \Delta G_s)}$$

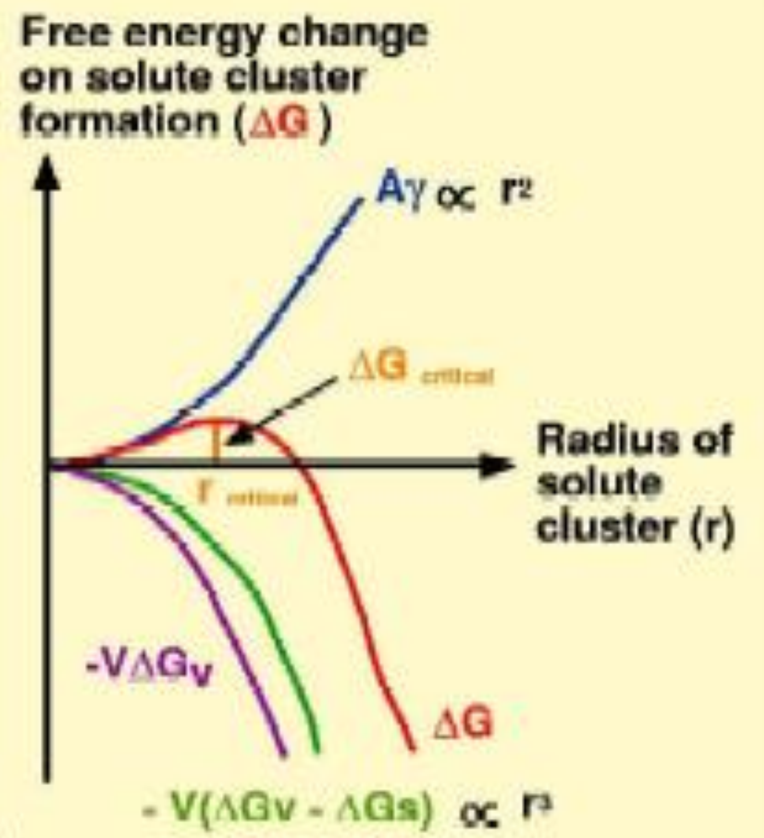

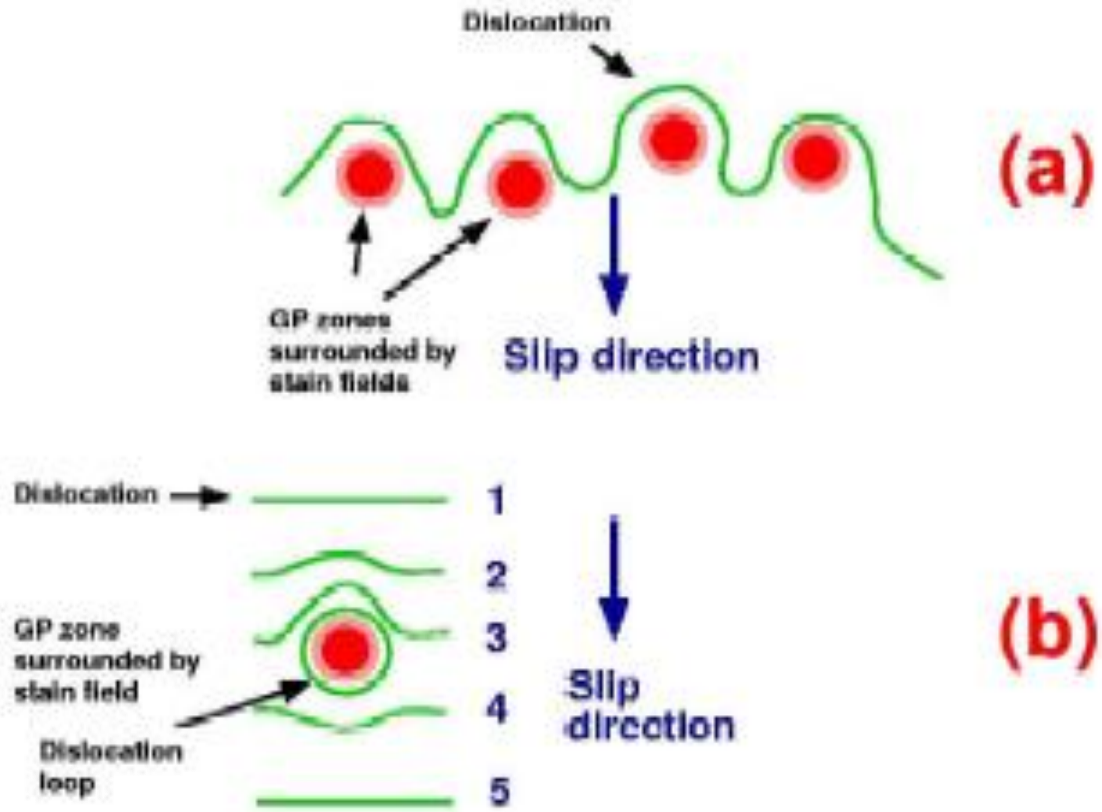

TALAT

GP zones resisting dislocation movement

1204.03.13

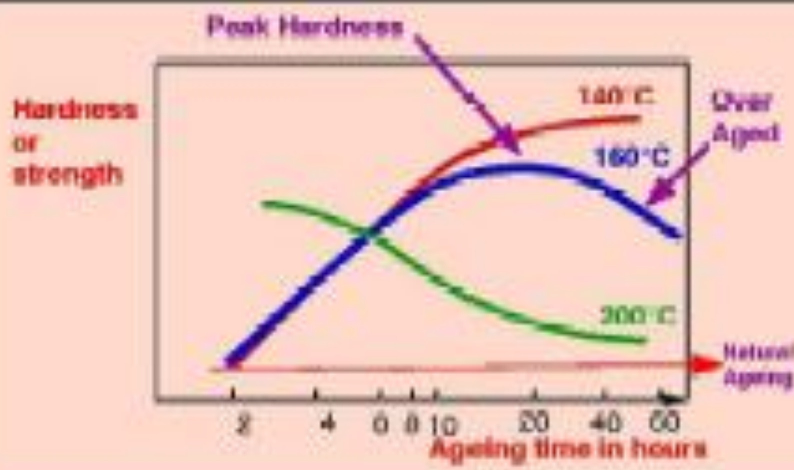

Shape of an ageing curve is determined by
(a) the alloy composition
(b) the quench rate
(c) the ageing temperature
(d) the nucleation rate
(e) the growth rate
(f) the rate of coarsening
(g) the precipitation sequence

Precipitate (cluster) nucleation rate (N) is given by

$$N = A \exp(-Q / kT) \exp(-\Delta G_{critical} / kT)$$

where
A is a constant
Q is the activation energy for diffusion

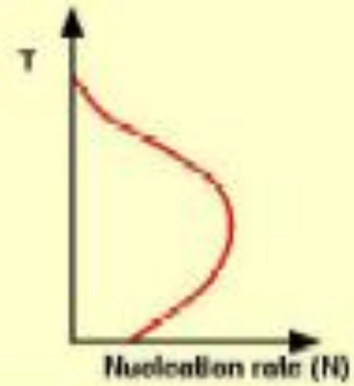

Grain boundary Precipitate-free Zone - solute depletion

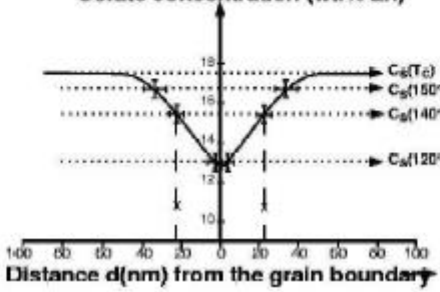

Direct quench into oil

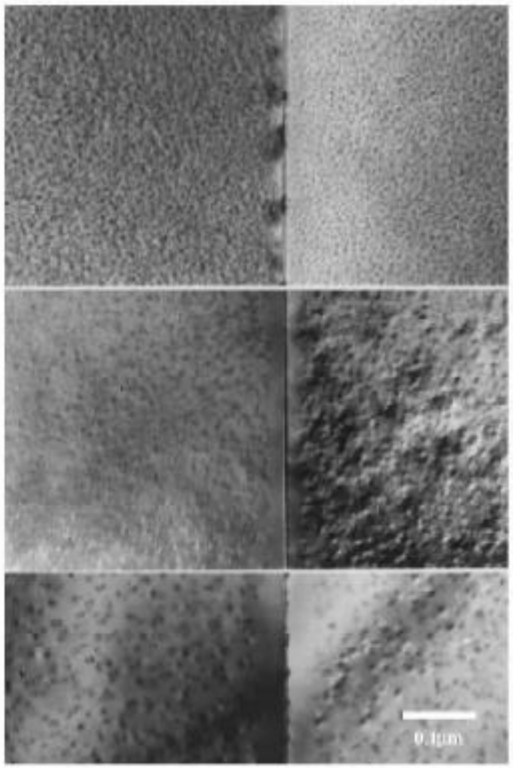

Aged at 120˚C for 2 hours

Aged at 140˚C for 2 hours

Aged at 150˚C for 1.5 hours

Grain boundary Precipitate-free Zones - vacancy depletion: Al-17.5%Zn

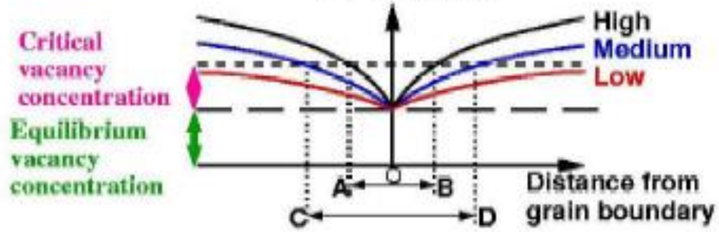

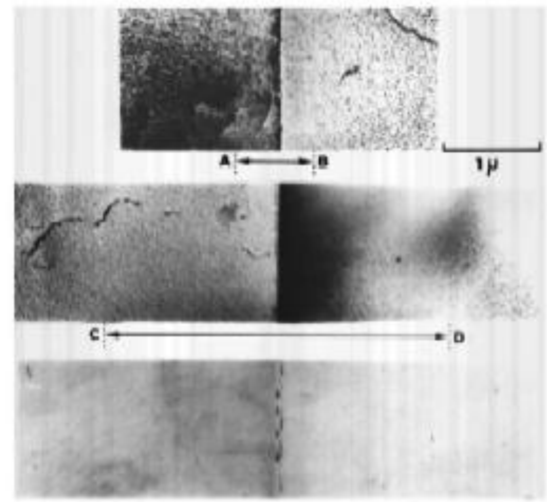

Al - 1.2% Mg_2Si : Heterogeneous precipitation on dislocations.
Quenched to 250˚C and held for 10 minutes + 6 months at room temperature + 24 hours at 160˚C.

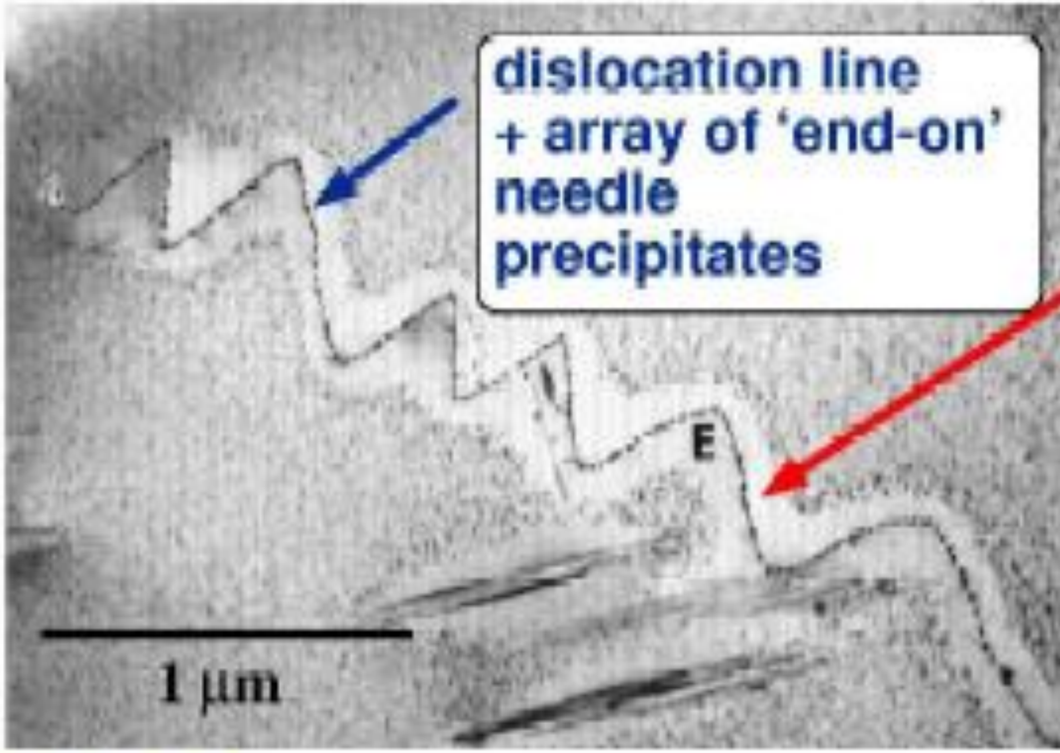

Note the region free of precipitates adjacent to the dislocation

Al - 1.2% Mg_2Si : Heterogeneous precipitation on dislocations.
Quenched to 250˚C and held for 10 minutes + 6 months at room temperature + 24 hours at 160˚C.

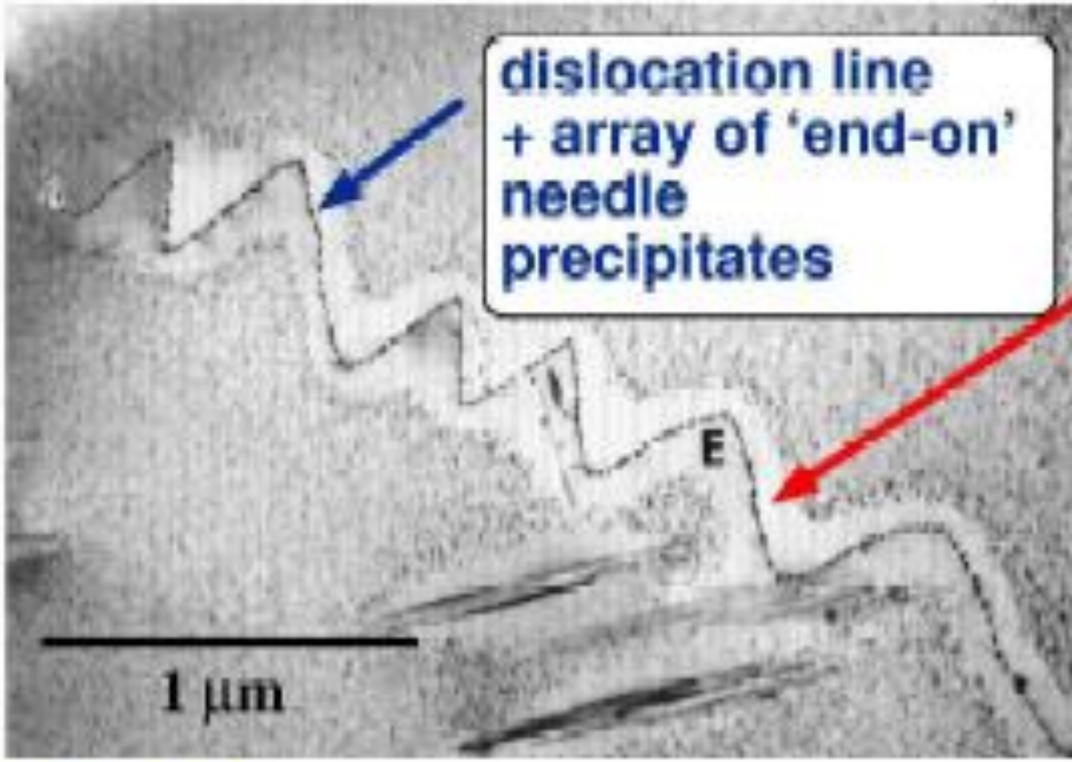

Note the region free of precipitates adjacent to the dislocation

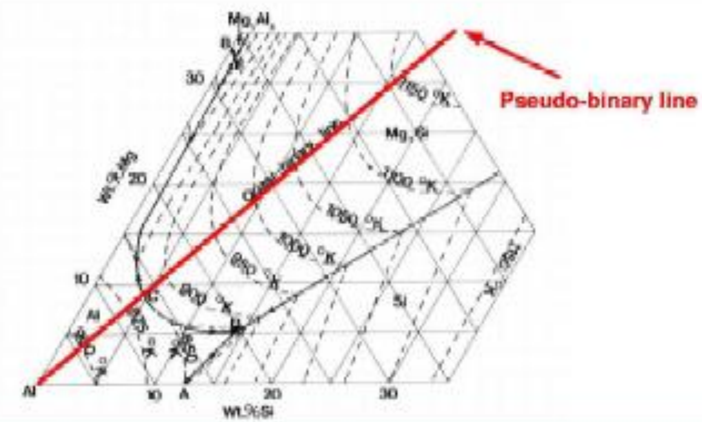

Liqidus surface at the aluminium- rich corner of the AlMgSi ternary phase diagram. The pseudo-binary line (also called the quasi-binary line) for Al-Mg_2Si is shown [after L E Mondolfo ref 4]

TALAT	Section of Al-Mg-Si ternary diagram	1203.02.02

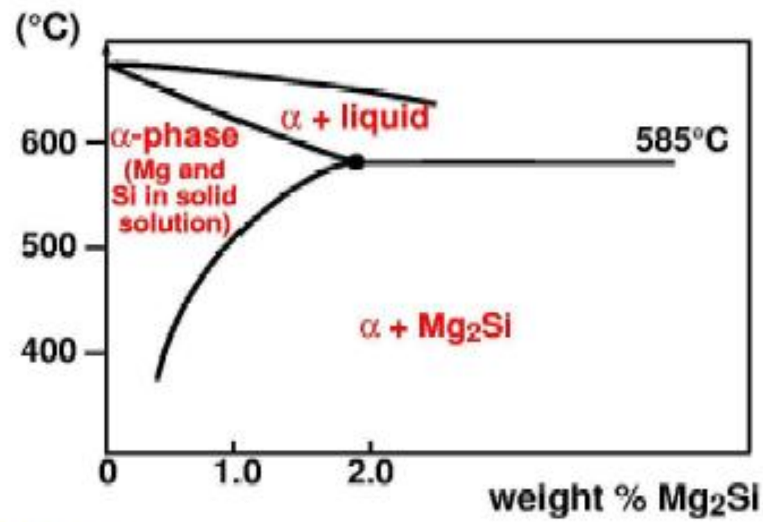

TALAT	Pseudo-binary section of Al-Mg-Si ternary diagram	1203.02.02

6013 alloy aged 8 hours at 165°C

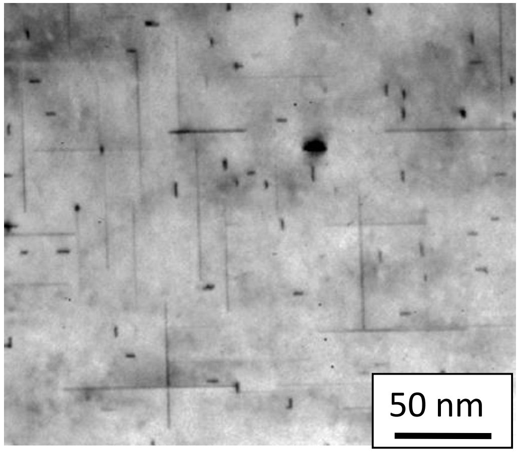

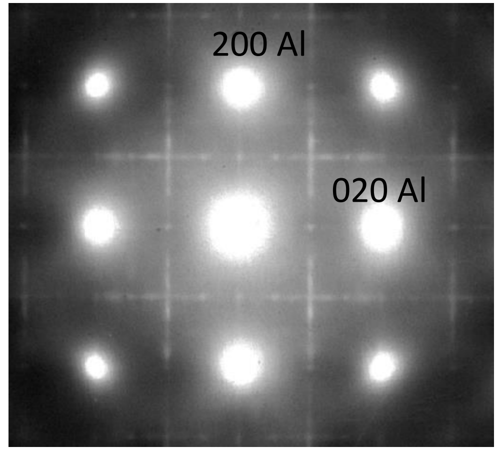

TEM bright image of and corresponding diffraction pattern with [001] Al zone axis.

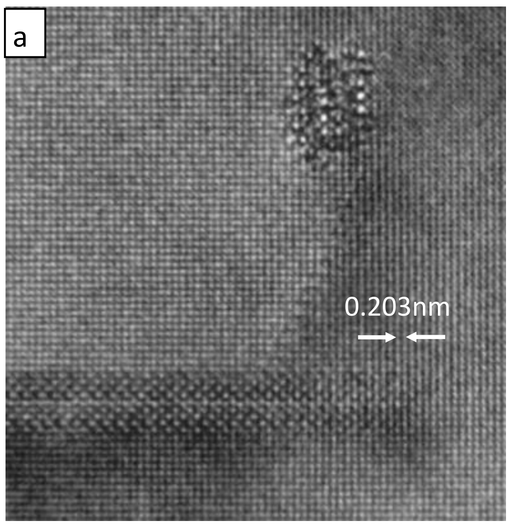

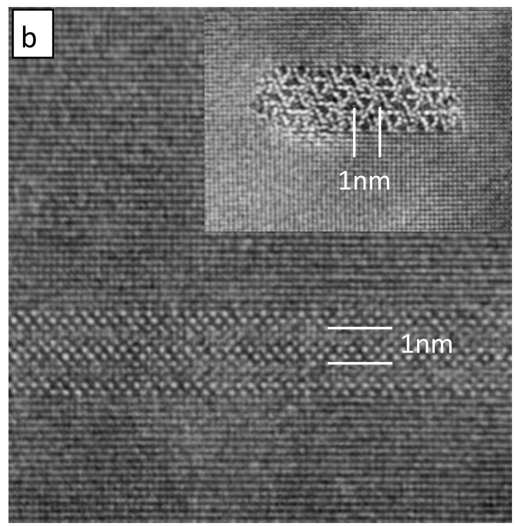

High resolution images of the precipitates

(a) the transition ordered phase;

(b) $Q(Al_5Cu_2Mg_8Si_7)$ precipitate and its cross section as an insert.

The microstructures contain fine uniformly dispersed rod-shape particles elongated in the <100>Al directions having rectangular or circular cross section. The streaks along <100>Al directions are attributed to shape effect of precipitates. The identification of the phases by SADP is difficult because of the similarity of diffraction patterns from different type of phases (β′, Θ′ or S′).

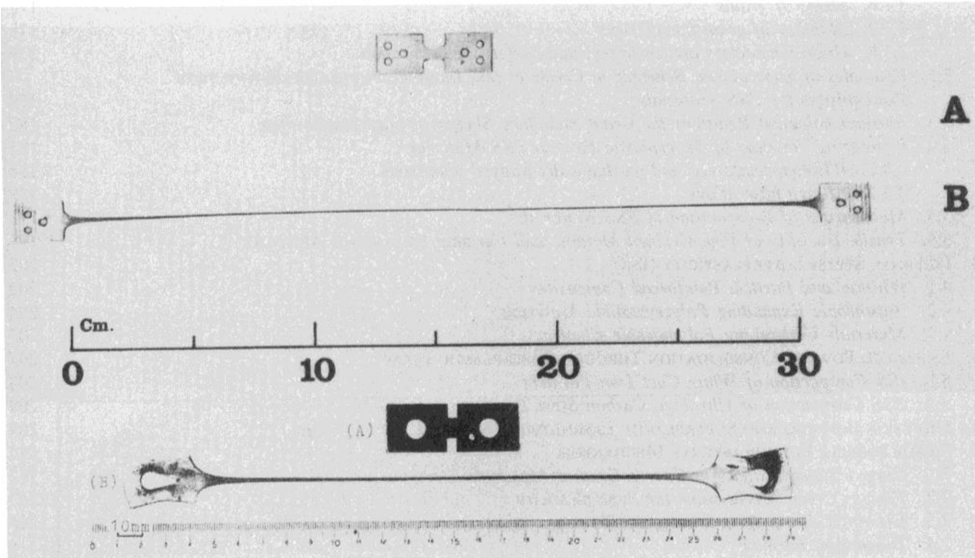

Superplastic elongation of 4850% in Pb-62%Sn alloy (A) after Ahmed and Langdon 1977 and 5500% in the sample of commercial alumnium bronze (B) after Higashi et al.. 1985

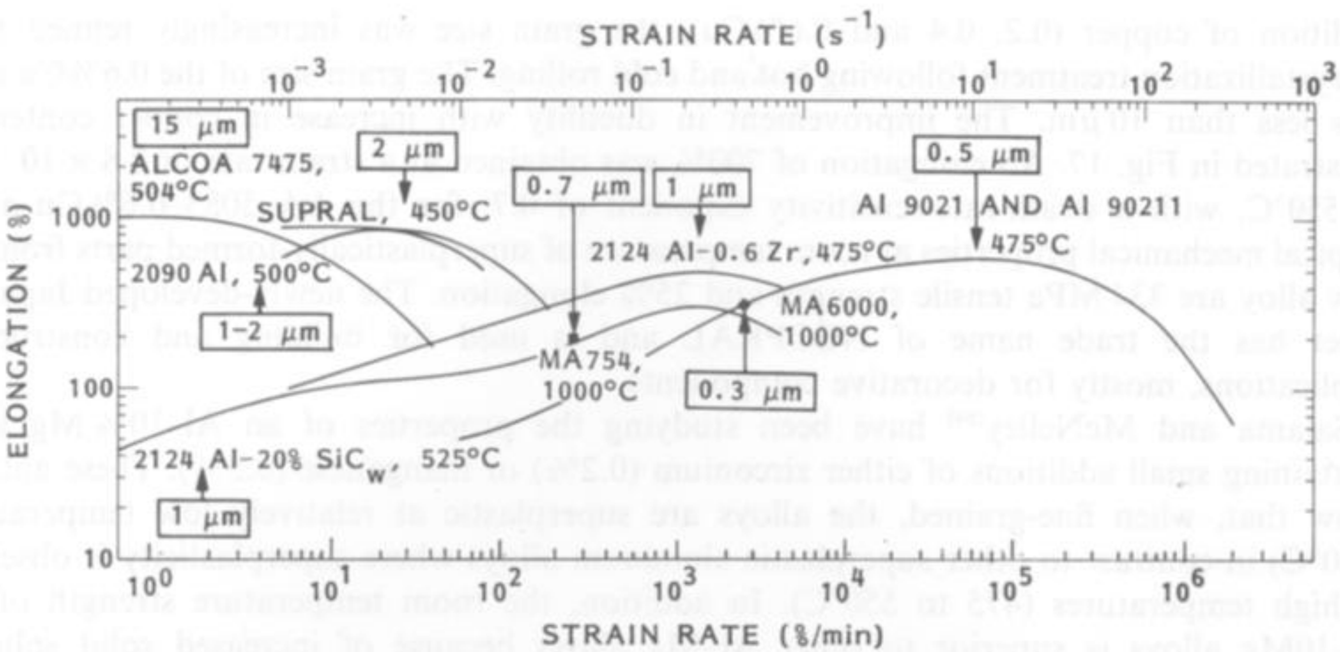

Overview of superplastic behavior as a function of strain rate for aluminium alloys of grain sizes from 15 µm to sub-micron. Included data points for Ni base alloys.

Superplastic Deformation of Aluminium Alloys

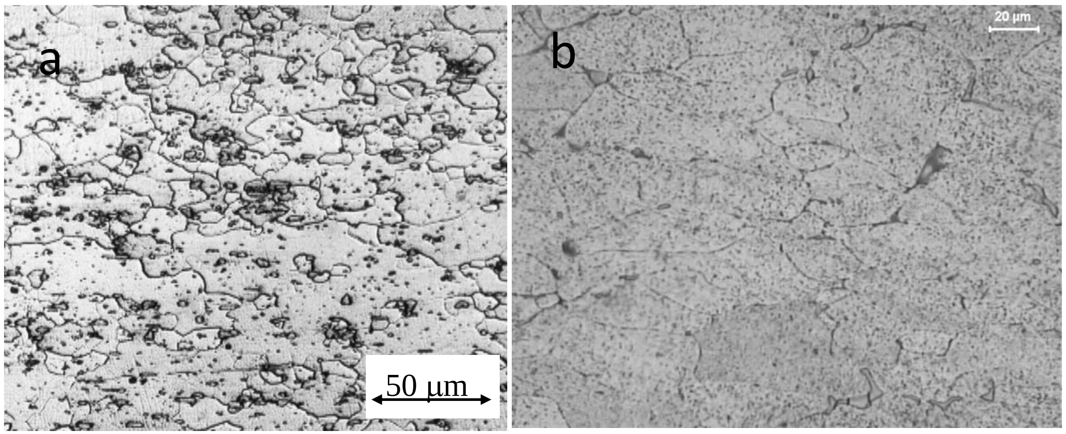

Optical microstructures of alloy AG2 continuously cast and hot rolled at 673K (a) and the same alloy cast to a copper mould AG2A (b)

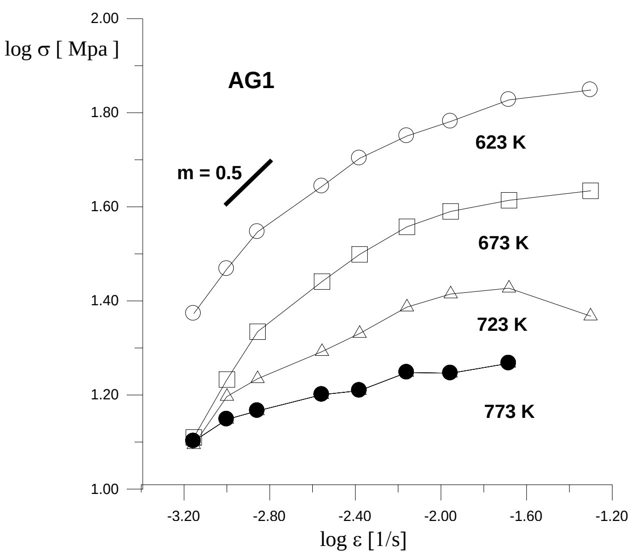

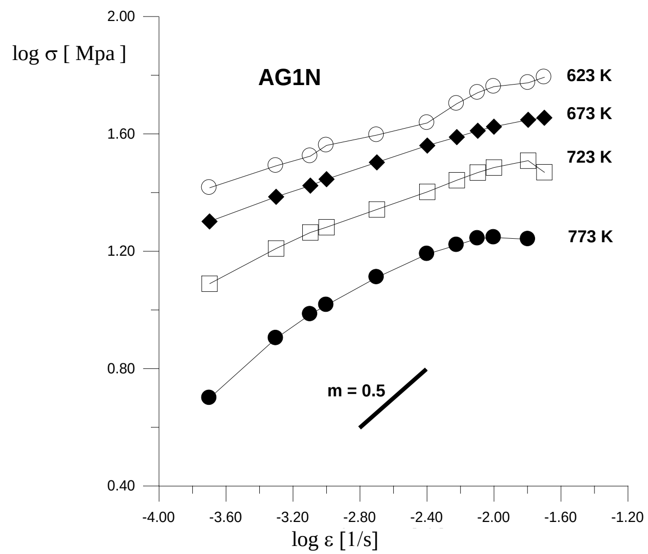

Relationship of tensile stress versus strain rate at temperatures 623K, 673K, 723K and 773 K obtained for the alloy AG1 and AG2.